A New Solvent Model for Hydrophobic Association in Water. 1. Thermodynamics

Teresa Head-Gordon

Contribution from the Life Sciences Division, Lawrence Berkeley Laboratory, University of California, Berkeley, California 94720

Received May 2, 1994[⊗]

Abstract: This work comprises the thermodynamic characterization of hydrophobic-water solutions using a recently introduced Hamiltonian of liquid water, which reproduces the short-ranged oxygen order while permitting all hydrogen bonding interactions to be isotropic. The thermodynamics of methane association is evaluated with this isotropic potential and compared to free energy simulations of methane-like groups in well-established models of liquid water where full anisotropy of hydrogen bonding is described. We find that the isotropic fluid reproduces the trends in free energy as a function of solute−water parameters, and that the free energy profiles appear to be quantitatively robust. The thermodynamic breakdown of the free energy indicates that the roles of entropy and enthalpy are reversed for quite small changes in the Lennard-Jones methane−solvent length parameter, σ, implying that molecular pictures of hydrophobic hydration based on reducing the exposed hydrophobic surface may be incomplete. This new Hamiltonian offers significant computational advantages and improved convergence of the thermodynamic components of the free energy when compared to the anisotropic water models. Furthermore, it offers a straightforward means for characterizing water as a solvent at different values of temperature and pressure.

1. Introduction

Hydrophobic hydration, interaction, and effect describes the observation that nonpolar groups tend to oppose their interaction with water with characteristic thermodynamic signatures which vary with temperature.[1−4] Hydrophobic hydration refers to the energetic and structural response of water near a single hydrophobic solute.[4−19] Hydrophobic interaction and effect describe the interaction of nonpolar groups with water, each other, and the interaction between solvent molecules themselves in the presence of two or more hydrophobic solutes.[20−30] These phenomena are peculiar to water alone as compared to other organic solvents. Any experiment or theory which attempts to explain hydrophobic behavior must discern the feature of liquid water that distinguishes it from other solvents.[4,30−32]

It has been suggested for many years that the hydrophobic effect involves water's optimization of its tetrahedral hydrogen bonding network around nonpolar solutes.[1−3] In this case water is distinguished by both its hydrogen bonding capabilities and preferred directions in which linear hydrogen bonds are formed. It is apparent that some loss of structural detail due to hydrogen bonding is tolerated when describing the thermodynamics of dissolution and association of nonpolar solutes in water, since scaled particle (SP) theory and its extensions[15−19] and the semiempirical Pratt−Chandler (PC) theories[20,22] are successful for predicting the thermodynamics of hydrophobicity. The description of water in these theories is the hard sphere radius of a water molecule in the case of SP theory (~1.35 Å being the empirically optimal value), or explicit inclusion of the

[⊗] Abstract published in *Advance ACS Abstracts,* December 1, 1994.

(1) Kauzmann, W. *Adv. Protein Chem.* **1959**, *14*, 1−63.
(2) Franks, F., Ed. *Water, A Comprehensive Treatise*; Plenum: New York, 1972−1982; Vols. 1−7.
(3) Ben Naim, A. *Hydrophobic Interactions*; Plenum: New York, 1980.
(4) For a review of the thermodynamics of hydrocarbon dissolution in water, see: Privalov, P. L.; Gill, S. J. *Adv. Protein Chem.* **1988**, *39*, 191−234.
(5) Owicki, J. C.; Scheraga, H. A. *J. Am. Chem. Soc.* **1977**, *99*, 7413−7418.
(6) Swaminathan, S.; Harrison, S. W.; Beveridge, D. L. *J. Am. Chem. Soc.* **1978**, *100*, 5705−5712.
(7) Mehrotra, P. K.; Mezei, M.; Beveridge, D. L. *J. Chem. Phys.* **1983**, *78*, 3156−3166.
(8) Jorgensen, W. L.; Gao, J.; Ravimohan, C. *J. Phys. Chem.* **1985**, *89*, 3470−73.
(9) Straatsma, T. P.; Berendsen, H. J. C.; Postma, J. P. M. *J. Chem. Phys.* **1986**, *85*, 6720−.
(10) Sheykhet, I.; Simkin, B. *J. Mol. Liq.* **1988**, *37*, 153−165.
(11) Jorgensen, W. L.; Blake, J. F.; Buckner, J. K. *Chem. Phys.* **1989**, *129*, 193.
(12) Pearlman, D. A.; Kollman, P. A. *J. Chem. Phys.* **1989**, *90*, 2460.
(13) Guillot, B.; Guissani, Y.; Bratos, S. *J. Chem. Phys.* **1991**, *95*, 3643−3648.
(14) Sun, Y.; Spellmeyer, D.; Pearlman, D. A.; Kollman, P. *J. Am. Chem. Soc.* **1992**, *114*, 6798−6801.
(15) Pierotti, R. A. *J. Phys. Chem.* **1965**, *69*, 281−288.
(16) Stillinger, F. H. *J. Soln. Chem.* **1973**, 2, 141−158.
(17) Pratt, L. R.; Pohorille, A. *Proc. Natl. Acad. Sci. U.S.A.* **1992**, *89*, 2995−2999.
(18) Pohorille, A.; Pratt, L. R. *J. Am. Chem. Soc.* **1990**, *112*, 5066−5074.
(19) Pratt, L. R.; Pohorille, A. *Proceedings of the EBSA, International Workshop on Water-Biomolecule Interactions 1992*; Palma, M. U., Palma-Vittorelli, M. B., Parak, F., Eds.; Societa' Italiana di Fisica: Bologna 1993.
(20) Pratt, L. R.; Chandler, D. *J. Chem. Phys.* **1977**, *67*, 3683−3704.
(21) Pangali, C.; Rao, M.; Berne, B. J. *J. Chem. Phys.* **1979**, *71*, 2975−2981.
(22) Pratt, L. R.; Chandler, D. *J. Chem. Phys.* **1980**, *73*, 3434−3441.
(23) Jorgensen, W. L.; Gao, J.; Ravimohan, C. *J. Phys. Chem.* **1985**, *89*, 3470−3473.
(24) Zichi, D. A.; Rossky, P. J. *J. Chem. Phys.* **1985**, *83*, 797−808.
(25) Jorgensen, W. L.; Buckner, J. K.; Boudon, S.; Tirado-Rives, J. *J. Chem. Phys.* **1988**, *89*, 3742−46.
(26) Laaksonen, A.; Stilbs, P. *Mol. Phys.* **1991**, *74*, 747−64.
(27) Smith, D. E.; Zhang, L.; Haymet, A. D. J. *J. Am. Chem. Soc.* **1993**, *114*, 5875−76.
(28) Smith, D. E.; Haymet, A. D. J. *J. Chem. Phys.* **1993**, *98*, 6445−6454.
(29) van Belle, D.; Wodak, S. J. *J. Am. Chem. Soc.* **1993**, *115*, 647−652.
(30) Ben-Naim, A. *J. Chem. Phys.* **1989**, *90*, 7412−7425.
(31) Dill, K. A. *Biochemistry* **1990**, *29*, 7133−7155.
(32) Baldwin, R. *Proc. Natl. Acad. Sci. U.S.A.* **1986**, *83*, 8069−8072.
(33) Narten, A. H.; Levy, H. A. *J. Chem. Phys.* **1971**, *55*, 2263−2269.

0002-7863/95/1517-0501$09.00/0

experimental two-body correlation of water oxygens determined by X-ray diffraction[34] in both extensions to SP theory[16] and PC theory.[20,22] All theories describe with increasing sophistication pertinent aspects of hydrogen bonding in liquid water, and literature[30] citing the failure of Pratt–Chandler theory as inadequate orientational descriptions of liquid water is inaccurate.

We have recently introduced a reference fluid which reproduces $g_{OO}(r)$ determined by neutron diffraction[35] (although reproducing x-ray experiment is equally possible), thereby providing a simplified approximation to the orientational components of hydrogen bonding. Φ_0 denotes this reference potential, while Φ_1 is the water interaction with explicit orientational degrees of freedom present. The perturbation from the Φ_0 reference state allowed us to examine the extent to which pure water properties depend upon the degree of orientational anisotropy of hydrogen bonding.[35] In this paper we explore the adequacy of Φ_0 for describing the thermodynamics of water solution phenomena involving hydrophobic solutes, as compared to traditional Φ_1 models. The success of SP[15] and PC[20,22] theories and subsequent analyses based on cavity distributions[16–19] already indicate that the Φ_0 potential should be a very good approximation to liquid water for describing hydrophobic-water solutions. In addition, it provides further advantages of a molecular description without the computational burden of Φ_1 model simulations incorporating explicit hydrogen bonding[21,23–29] and greatly broadens the scope of simple model descriptions beyond the analytic SP and PC theories.[15–20,22]

Our foremost objective is to demonstrate that our computationally simple reference fluid Hamiltonian, Φ_0, captures the relevant physics for describing the hydrophobic interaction and effect. We will show that the reference fluid described above appears to accurately describe the trends in free energy profiles for small solute association at relative distances of 8 Å or less, as compared to PC theory[20] and reported simulations using the more computationally expensive Φ_1 water models.[21,23–29] Secondly, the nature of the reference fluid interactions is such that the thermodynamic breakdown of the free energy into enthalpic and entropic contributions is much improved when compared to their simulation using Φ_1 models for a given system size.[27,28] While we have not fully exploited the convergence advantage in this work, we still can report on the qualitative breakdown of the free energy, throughout the investigated range in relative methane separation, and for all solute–water parameters studied. Only one simulation study has reported the enthalpic and entropic components of the free energy of hydrophobic association (using the SPC Φ_1 model and 106 waters), and only in the free energy region where the groups are in contact.[27,28] The thermodynamic breakdown into enthalpic and entropic components for simulations using our reference fluid as solvent is also consistent with this work.[27,28] Furthermore, we report on a reversal of entropic and enthalpic roles as the methane–water interaction length parameter is decreased, which suggests that molecular pictures based solely on exposed surface areas of the solutes may be incomplete.[1–3,27,28]

Section 2 provides details of the computational procedures and potential functions used to generate the potential of mean force (pmf) profiles presented in Sections 3 and 4. We conclude in Section 5 with plans for research in the immediate future.

Table 1. Parameters for Reference Fluid Potential[a]

parameter	HNC	parameter	HNC	parameter	HNC	parameter	HNC
a	12.0000	c_1	2.8443	w_1	0.2498	h_1	−1.0978
b	6.0000	c_2	4.4947	w_2	−0.7738	h_2	−0.3466
ϵ	0.0050	c_3	0.0767	w_3	2.0806	h_3	11.2701
σ	3.1000	c_4	6.4928	w_4	−1.2480	h_4	−0.2009

[a] Energy units are kcal/mol.

2. Theory and Methods

No quantum effects have been incorporated into the molecular dynamics simulations of water solutions,[36] nor descriptions of solvent polarization.[29] While quantum effects are known to be significant in describing water structure,[36] the classical potentials describing the two perturbation endpoints have been shown to reproduce the structural short-ranged order as described by the (inherently) quantum mechanical neutron diffraction data.[34] With respect to many-body effects, recently reported free energy profiles for methane association in water have indicated that explicit inclusion of water polarization eliminates the solvent-separated minimum.[28] While this study has demonstrated that polarization may be quantitatively important, it does not incorporate a description of solute–water polarization. A strengthening of the solute–solvent interaction may very well re-stabilize the solvent-separated minimum and modify conclusions based on its purported annihilation.[29] We note that there is some uncertainty in the best methane–water Lennard-Jones parameters as well, where smaller σ_{MeO} and larger ϵ_{MeO} further stabilize the solvent-separated minimum.[20,22,28]

Potential Functions. The design of the reference fluid is discussed elsewhere,[23] and only a brief outline of that procedure is given here. The Ornstein–Zernike (OZ) equation,[37]

$$h(r) = c(r) + \varrho \int c(\mathbf{r} - \mathbf{r}')\, h(\mathbf{r}')\, d\mathbf{r}' \tag{2.1}$$

provides an exact relation between the radial distribution function, $g(r) = h(r) + 1$, the direct correlation function, $c(r)$, and the density, ϱ. By manipulating the OZ equation and using the experimentally determined oxygen–oxygen radial distribution function, we can isolate the direct correlation function, $c(r)$. The hypernetted chain (HNC) approximation,[37]

$$\phi(r) = k_b T\{g(r) - 1 - \ln[g(r)] - c(r)\} \tag{2.2}$$

and both $g_{OO}(r)$ and $c(r)$ allowed us to define an isotropic reference fluid, where $\phi(r)$ represents a generic pair potential, k_b is Boltzmann's constant, and T is the temperature. The resulting tabulated potential was fit to the following functional form:

$$\Phi_0(r) = \epsilon[(\sigma/r)^a - (\sigma/r)^b] + \sum_{i=1}^{4} h_i \exp[-(r - c_i)^2/w_i^2] \tag{2.3}$$

and Monte Carlo simulations using (2.3) established the validity of the HNC approximation by reproducing the experimental pair distribution function to within statistical error.[35] As discussed previously, the PY closure[38] did very poorly in this respect,[35] but its performance in describing water solutions should be further explored. All HNC parameters for eq 2.3 are tabulated in Table 1. In order to optimize the execution time in evaluating $\Phi_0(r)$ and its derivative, we have refit the potential so that the first term in eq 2.3 is a 6–12 Lennard-Jones function. The resulting parameters listed in Table 1 are therefore different from our previous work,[35] but both potentials produce the same radial and angle distribution functions.[34,35]

Many liquid water potentials are available for approximating Φ_1.[35,39–42] Because we wish to separate the orientational component of hydrogen bonding from that which gives rise to local oxygen order,

(34) Soper, A. K.; Phillips, M. G. *Chem. Phys.* **1986**, *107*, 47–60.
(35) Head-Gordon, T.; Stillinger, F. H. *J. Chem. Phys.* **1993**, *98*, 3313–27.
(36) Kuharski, R. A.; Rossky, P. J. *J. Chem. Phys.* **1985**, *82*, 5164–5177.
(37) Hansen, J. P.; McDonald, I. R. *Theory of Simple Liquids*; Academic Press: London, 1986.
(38) Percus, J. K.; Yevick, G. J. *Phys. Rev.* **1958**, *110*, 1.
(39) Stillinger, F. H.; Rahman, A. *J. Chem. Phys.* **1974**, *60*, 1545–1557.

Table 2. Parameters for the ST4 Potential

parameter	ST4	parameter	ST4
ϵ (kcal/mol)	0.07575	θ_{H-O-H} (deg)	109.4700
σ (Å)	3.10000	$\theta_{LP-O-LP}$ (deg)	134.4700
$q_H = -q_L$ (e)	0.24570	R_L (Å)	2.01600
r_H (Å)	1.00000	R_U (Å)	3.12870
r_{LP} (Å)	0.80000		

we desire a full water potential which, like the reference fluid, best reproduces the experimental $g_{OO}(r)$.[42] The ST4 water potential,[35] a minor variant on its venerable ST2 predecessor,[39] was specifically designed for that purpose. The functional form of ST2 and ST4 is[39]

$$V_I(1,2) = V_{LJ}(r) + S(r)\, V_{el}(1,2) \tag{2.4}$$

where r is the distance between water molecule oxygens, V_{LJ} is the standard Lennard-Jones function which depends on the oxygen−oxygen separation only,

$$V_{LJ}(r) = 4\epsilon[(\sigma/r)^{12} - (\sigma/r)^6] \tag{2.5}$$

and V_{el} designates Coulomb's law evaluated for all 16 intermolecular charge interactions in the model. $S(r)$ is a modulating function which interpolates smoothly between 0 and 1 and is applied to the charge interaction in order to avoid electrostatic catastrophes exhibited by some relative orientations of a pair of water molecules.[39]

$$S(r) = 0 \qquad 0 \le r \le R_L$$

$$S(r) = \frac{(r - R_L)^2(3R_U - R_L - 2r)}{(R_U - R_L)^3} \qquad R_L \le r \le R_U$$

$$S(r) = 1 \qquad r \ge R_U \tag{2.6}$$

The parameters for ST4 are given in Table 2.[35] The two hydrophobic solutes interact with each other and with water through a Lennard-Jones potential (eq 2.5). We have investigated a number of solute−water interaction strength parameters in order to understand how this interaction influences the potential of mean force profiles. The solute may be viewed as an approximation to methane. All parameters relating to the hydrophobic groups are clearly discussed in the remainder of the text.

Long-Ranged Interactions. We report $\lambda = 1.0$ simulation results using both energy and force truncation and Ewald sums[43] to describe the long-ranged interactions. Equation 2.6, used to modify short-ranged electrostatic interactions described in the previous paragraph, was also used to modify the long-ranged forces by reversing the roles of R_U and R_L. In this case, the values of R_U and R_L were 8.13 and 9.13 Å, respectively. When Ewald sums were evaluated, the electrostatic potential now takes the form[43]

$$V_{el} = \frac{1}{2}\sum_i^N \sum_j^N \left(\sum_{|\mathbf{n}|=0}^{\infty}{}' q_i q_j \frac{\mathrm{erfc}(|\mathbf{r}_{ij} + \mathbf{n}|)}{|\mathbf{r}_{ij} + \mathbf{n}|} + (4\pi/L^3) \sum_{\mathbf{k}\neq 0}^{\mathbf{k}_m} q_i q_j \frac{1}{k^2} (e^{-k^2/4\kappa^2} e^{-i\mathbf{k}\tau_{ij}}) \right) - \sum_i^N \sum_m^M q_{im} (2\kappa q_{im}/\pi^{1/2} + \sum_n^M q_{in}\, \mathrm{erf}(\kappa r_{mn}{}^i)/r_{mn}{}^i) \tag{2.7}$$

where a Gaussian form for the modified charge distribution is assumed. We have used a convergence parameter $\kappa = 6.0/L$ and truncated the k-space sum at $k_m = 3$. We note that complex variables reduce the computation of the k-space sum to a scaling of $k_m{}^3N$, where N is the number of interaction sites.[43] The evaluation of the r-space sum was truncated at $\mathbf{n} = \mathbf{0}$, and the minimum image convention was used to evaluate all real space interactions. In the case of the reference fluid, all solvent−solvent interactions were evaluated with the minimum image convention. The minimum image convention was also used for evaluating the solute−solvent interactions for both the $\lambda = 0$ and 1 simulations.

Simulation Details. The velocity Verlet algorithm[44] was used to integrate the equations of motion for 214 molecules and two fixed hydrophobic groups approximating methane, at the thermodynamic point 298 K, 1 atm, and 1 kg/L. A timestep of 1.5 fs was used for all reported calculations involving ST4, and 2.0 fs was used for the reference fluid. The simulation length for the reference fluid comprised 30 ps of equilibration and 60 ps of dynamics for each pmf window. For our model of methane in ST4 water, each pmf window was equilibrated at 45.0 ps and averages were accumulated during a subsequent 75.0 ps simulation. For one ST4 simulation with $\sigma_{MeO} = 3.445$ Å, $\epsilon_{MeO} = 0.3134$ kcal/mol, and using Ewald sums, averages were accumulated during 112.5 ps of dynamics for each window. Constant temperature was maintained by periodically (every 1.5 ps) rescaling velocities. When explicit hydrogen bonding is present ($\lambda \neq 0$). RATTLE[45] was used to maintain the rigidity of the ST4 internal degrees of freedom.

The potential of mean force (pmf) profiles presented in the following sections were derived from the above described molecular dynamics protocol in the NVT ensemble using statistical mechanical perturbation in the relative methane−methane separation, r.[46]

$$\Delta A = -k_b T \ln\langle e^{-\beta(U(r+\Delta r) - U(r))}\rangle_0 \tag{2.8}$$

where U is the configurational energy, and subscripts denote averages in the unperturbed ensemble. Simulations were performed in the range of discrete methane−methane separations between 3.375 and 7.875 Å, and each simulation covered 0.25 Å (a perturbation of ±0.125 Å). In addition to the free energy, we have also evaluated the enthalpic and entropic contributions using a fluctuation formula method.[13,28] The enthalpy is evaluated according to

$$\Delta E = \frac{\langle U(r + \Delta r) e^{-\beta[U(r+\Delta r) - U(r)]}\rangle_0}{\langle e^{-\beta[U(r+\Delta r) - U(r)]}\rangle_0} - \langle U(r)\rangle_0 \tag{2.9}$$

and the entropic piece is derived from $\Delta A - \Delta E$.

3. Thermodynamics of Methane Association in Fully Coupled ST4 Water

This section provides a benchmark simulation of methane association in the ST4 Φ_1 model of water (full hydrogen bonding present) for comparison with the reference fluid simulations described in the next section. We have used the ST4 model[35] for two reasons. Originally, we wanted to use a Φ_1 model designed to reproduce the $g_{OO}(r)$ determined from neutron diffraction data[34] on liquid water at 298 K and 1 atm, thereby providing the cleanest means for discerning the influence of orientational preferences of hydrogen bonding.[35] In addition, we wanted to estimate the precision with which the free energy could be determined based on differences among water models and long-range force considerations.[21,23−28] The pmf's generated from the same set of methane-water Lennard−Jones parameters, but different water models and treatment of long-ranged forces, show some differences in the relative energies of the contact and "solvent-separated" minima.[25,27,28] We thought further calculations involving a different water model and varying the

(40) Berendsen, H. J.; Postma, J. P. M.; van Gunsteren, W. F.; Hermans, J. In *Intermolecular Forces*; Pullman, B., Ed.; Reidel: Dordrecht, 1981.
(41) Jorgensen, W. L.; Chandrasekhar, J.; Madura, J. D.; Impey, R. W.; Klein, M. L. *J. Chem. Phys.* **1983**, *79*, 926−935.
(42) Watanabe, K.; Klein, M. L. *Chem. Phys.* **1989**, *131*, 157−167.
(43) Allen, M. P.; Tildesley, D. J. *Computer Simulation of Liquids*; Clarendon Press: Oxford, 1987.
(44) Anderson, H. C. *J. Chem. Phys.* **1980**, *72*, 2384−.
(45) Andersen, H. C. *J. Comp. Phys.* **1983**, *52*, 24−34.
(46) Mezei, M.; Beveridge, D. L. *Ann. N.Y. Acad. Sci.* **1986**, *482*, 1−23.

Table 3. Thermodynamics of Methane Association in the Reference Fluid and ST4

λ fluid[a]	σ_{MeO}[b]	ϵ_{MeO}[c]	ΔA_{min}[c,d]	ΔA_{bar}[c,e]
0.0 (M)	3.445	0.2134	-0.31 ± 0.02	0.28 ± 0.02
0.0 (M)	3.445	0.3134	-0.63	0.33
0.0 (M)	3.550	0.2134	-0.22	0.53
0.0 (M)	3.550	0.3134	-0.13	0.65
0.0 (M)	3.650	0.2134	0.33	0.87
0.0 (M)	3.650	0.3134	0.05	0.98
1.0 (E)	3.445	0.2134	0.53 ± 0.03	1.00 ± 0.03
1.0 (E)	3.650	0.2134	0.39	1.04
1.0 (E)	3.445	0.3134	0.36	0.79 ± 0.03
1.0 (T)	3.445	0.3134	0.25	0.73

[a] Denotes type of solvent model (see text) and solvent–solvent interaction evaluation method: M = minimum image, E = Ewald sums, T = energy and force truncation. [b] In units of Å. [c] In units of kcal/mol. [d] "Min" denotes maximum free energy difference in the vicinity of the solvent separated and contact minimum. All simulations for a given λ value had comparable error bars. [e] "Bar" denotes maximum free energy difference in the vicinity of the barrier and contact minimum. All free energies for a given λ value have comparable error bars.

method of evaluating long-ranged forces might provide a more complete set of data to determine where the error might lie in these quantitative differences.

There is some uncertainty in the best value of both σ_{MeO} and ϵ_{MeO}, and values ranging from 3.2 to 3.445 Å and from 0.2134 to 0.3320 kcal/mol, respectively, have been used.[23-28] While these parameters may be deduced from simple mixing rules of the Lennard-Jones parameters with any of the existing Φ_1 water potentials, there is still some ambiguity in the effective molecular size of an associated fluid such as water. This problem is well-illustrated with our reference fluid, eq 2.3, since various σ_{OO} and ϵ_{OO} could, with appropriate adjustment of the remaining parameters, reproduce the radial distribution function. We return to this point in the next section when we compare simulations using the reference fluid and the ST4 Φ_1 water model. The methane–oxygen parameters we have investigated using the ST4 model are $\sigma_{MeO} = 3.445$ Å and $\epsilon_{MeO} = 0.2134$ and 0.3134 kcal/mol. We have also considered a larger σ_{MeO} of 3.65 Å as compared to previous work. Table 3 contains tabulated relative free energies between the minima and between the contact minimum and barrier for all simulations reported in this section and Section 4.

The $\sigma_{MeO} = 3.445$ Å and $\epsilon_{MeO} = 0.2134$ kcal/mol set of methane–oxygen parameters have been used by a number of researchers,[25-28] and Figure 1a displays the free energy of association using the ST4 model solvent with this same set. The zero of energy has been placed at $r = 7.875$ Å, the maximum distance studied. The ST4 simulation finds the contact minimum to be more stable (assuming equal populations) than the solvent-separated minimum, with a barrier of ~1 kcal/mol separating them. Differences among reported simulations pertain to the relative energies of the two minima; as in a recent study using the SPC water model and Ewald sums,[27,28] we find the relative energy difference to be ~0.55 kcal/mol. We therefore might indirectly infer that differences among water models are not responsible for a smaller relative energy (0.25–0.4 kcal/mol) found by a recent study using TIP4P,[25] although we cannot rule out this possibility.

As originally predicted by Pratt and Chandler,[22] increasing ϵ_{MeO} will result in an increasing preference for the solvent-separated minimum. Figure 2a shows the free energy curves for $\epsilon_{MeO} = 0.3134$ kcal/mol for the methane–solvent length parameter of 3.445 Å, using Ewald sums. When the relative energies in Table 3 are compared, it is evident that the ST4 model also captures this trend. We have also evaluated the free

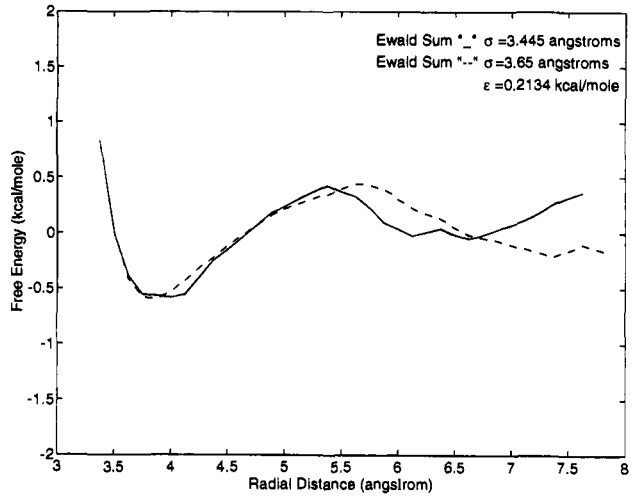

Figure 1. The free energy of methane association in the Φ_1 ST4 model of water with varying values of σ_{MeO}: (a) —, $\sigma_{MeO} = 3.445$ Å, $\epsilon_{MeO} = 0.2134$ kcal/mol, Ewald sums; (b) - - -, $\sigma_{MeO} = 3.65$ Å, $\epsilon_{MeO} = 0.2134$ kcal/mol, Ewald sums.

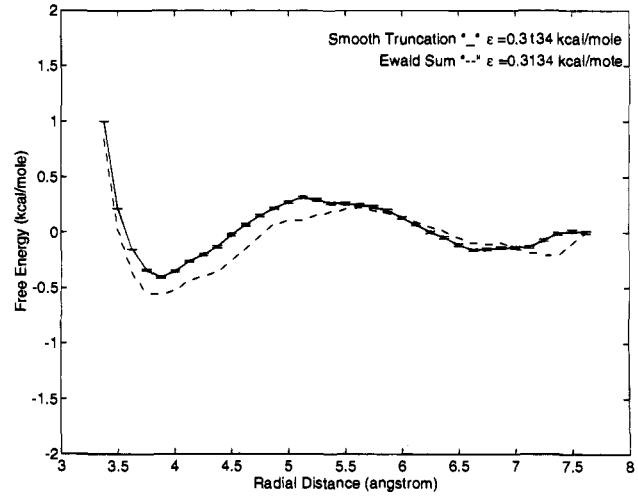

Figure 2. The free energy of methane association in the Φ_1 ST4 model of water. The Φ_1 simulations have been examined with a different value of ϵ_{MeO} than in Figure 1, and two different approximations of long-ranged forces: (a) —, $\sigma_{MeO} = 3.445$ Å, $\epsilon_{MeO} = 0.3134$ kcal/mol, Ewald sums; (b) - - -, $\sigma_{MeO} = 3.4455$ Å, $\epsilon_{MeO} = 0.3134$ kcal/mol, energy and force truncation.

energy of association for this same set of methane–water parameters using the energy-force truncation scheme described in Section 2 (Figure 2b). As is evident from Table 3, there is a small difference in the pmf profiles at the contact minimum due to differences in the methods for treating long-ranged forces. This difference, ~0.15 kcal/mol, partly explains the discrepancy between calculations reported by Jorgensen et al.[25] and Smith and Haymet.[27,28] It is possible that the remaining energetic difference of ~0.2 kcal/mol may be due to convergence differences between Metropolis Monte Carlo as compared to Newtonian molecular dynamics, although the influence of a different water model on the free energy is still possible.

We have also investigated changes in σ_{MeO} as well, where previous simulation studies[21,23-28] have clearly demonstrated that increasing the interaction length parameter results in an increasing preference for the contact minimum. Reported simulations indicate that there is a qualitative shift in the relative minima ordering between σ_{MeO} values of 3.2 and 3.445 Å, where the former value favors the solvent-separated minimum while the latter value shows a contact minimum preference. The

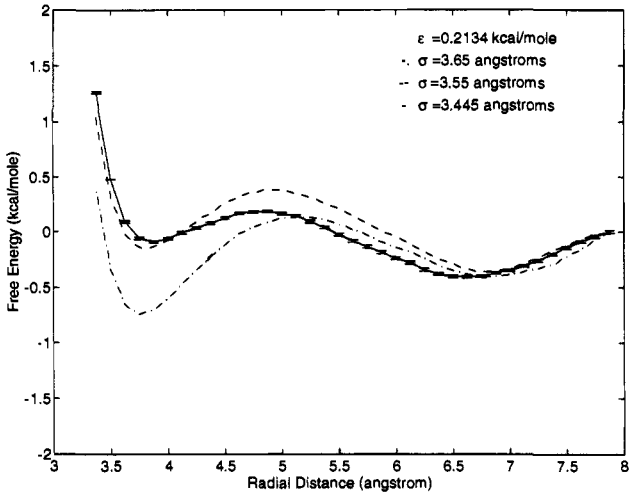

Figure 3. The free energy of methane association in the $\lambda = 0.0$ reference fluid for $\epsilon_{MeO} = 0.2134$ kcal/mol and varying the σ_{MeO} interaction length parameters: (a) —, $\sigma_{MeO} = 3.445$ Å, (b) - - -, $\sigma_{MeO} = 3.55$ Å, and (c) - · -, $\sigma_{MeO} = 3.65$ Å.

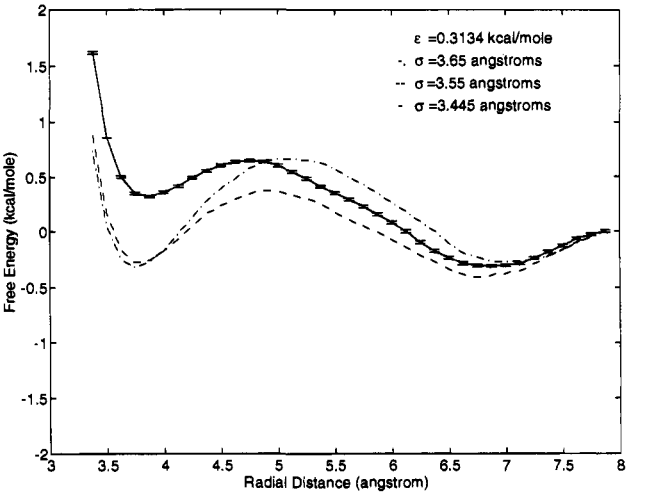

Figure 4. The free energy of methane association in the $\lambda = 0.0$ reference fluid for $\epsilon_{MeO} = 0.3134$ kcal/mol and varying the σ_{MeO} interaction length parameters: (a) —, $\sigma_{MeO} = 3.445$ Å, (b) - - -, $\sigma_{MeO} = 3.55$ Å, and (c) - · -, $\sigma_{MeO} = 3.65$ Å.

position of the barrier and solvent-separated minimum shift outward as σ_{MeO} increases, with the solvent-separated minimum consistently positioned at twice the value of σ_{MeO}. To extend the existing data set, and for purposes involving the next section, we have also evaluated the free energy using a larger value of σ, while retaining some approximation to methane, using $\sigma_{MeO} = 3.65$ Å and $\epsilon_{MeO} = 0.2134$ kcal/mol. Figure 1b compares this set of data to the free energy evaluated using a smaller σ_{MeO} value of 3.445 Å. The positions of the barrier and solvent-separated minimum have shifted as expected, although relative free energies (Table 3) have changed little. Therefore within a fairly narrow window of σ_{MeO} values ranging from 3.2 to 3.65 Å, we see a reversal of free energy trend occurring at $\sigma_{MeO} = \sim 3.445$ Å. Apparently larger σ_{MeO} favors release of solvent to the bulk, but it is unclear whether this is due to nonoptimal packing of the solvent around the solutes or poor interactions among solvent particles themselves in the first, and possibly second, solvation shells.

While error bars for the free energy are small ($\sim \pm 0.02$ kcal/mol), we found it difficult to converge the enthalpic and entropic components of the free energy with our ST4 simulation using 214 water molecules. The study by Smith and Haymet, using 106 water molecules, is the only one we are aware of which evaluated the free energy breakdown for methane association.[27,28] Their results at the turnover point in σ_{MeO} described above indicate that the formation of the contact minimum is entropically driven, in accordance with traditional views of hydrophobicity where ice-like structure (and unfavorable entropy) is minimized by minimizing exposed solute surface area to water (solutes in contact instead of solvent separated).[1-3,27,28] In the next section we will demonstrate that all trends discussed in this section are reproduced with Φ_0 as well and draw new conclusions about the solvent-induced driving forces for methane association as σ_{MeO} is varied.

4. Thermodynamics of Methane Association in the Reference Fluid

Figure 3a displays our calculated potential of mean force between two Lennard-Jones spheres approximating methane in the $\lambda = 0$ reference fluid, using the most commonly employed methane–water interaction parameters of 0.2134 kcal/mol and 3.445 Å.[25,27,28] The zero of energy has been placed at the maximum distance studied. Unlike the Φ_1 models described in Section 3, including our benchmark calculation using the ST4 model, the reference fluid using this particular set of methane–water parameters instead shows a preference for the solvent-separated minimum. In fact, our free energy curve resembles quite closely results found by Pratt–Chandler theory[20] and other simulation studies using $\sigma_{MeO} = 3.2$ Å.[27,28] This would imply that increasing the methane–water interaction length parameter should reverse this trend in the relative energies to eventually favor the contact minimum.[27,28]

This is the case in practice. As σ_{MeO} is increased to 3.55 (Figure 3b) and to 3.65 Å (Figure 3c) with ϵ_{MeO} fixed at 0.2134 kcal/mol, the forward barrier separating the contact minimum from the solvent-separated minimum becomes larger, and the position of the barrier and solvent-separated minimum moves to larger r. At $\sigma_{MeO} = 3.65$ Å we see the reversal in the free energy ordering of the two minima, so that at this methane–reference fluid interaction length value the contact minimum is preferred. The actual quantitative comparison of the free energy profiles between our reference fluid using $\sigma_{MeO} = 3.65$ Å and the Φ_1 models using $\sigma_{MeO} = 3.445$ Å is quite reasonable, although a further small increase of σ_{MeO} would improve quantitative agreement. The necessity of increasing the solute–solvent interaction length suggests that explicit hydrogen bonding influences the release of solvent to the bulk for smaller solute–solvent interaction lengths than the reference fluid. We return to this point in the next section. Nonetheless, the reference fluid does reproduce the same trends exhibited in the pmf profiles simulated using various Φ_1 models as σ_{MeO} increases.[21,23-28] In fact, these calculations and the additional results described below indicate that the choice of σ_{MeO} in the reference fluid is a small, systematic correction to the full hydrogen bond results.

In addition to pmf changes due to σ_{MeO}, there are well-appreciated free energy trends observed as ϵ_{MeO} is varied as well.[22] These are less dramatic than changes in σ_{MeO}, although they are still observable. We expect that as ϵ_{MeO} is increased, the two solutes separated by one water layer will allow for a greater number of more favorable solute–water interactions, which may eventually overcome the unfavorable entropy for water structuring around this greater solute surface area.[22] Briefly stated, the reference fluid reproduces this trend as well (Figure 4), regardless of the σ_{MeO} value employed.

Figures 5 and 6 portray the calculated enthalpic and entropic components to the free energy, for $\epsilon_{MeO} = 0.2134$ kcal/mol and

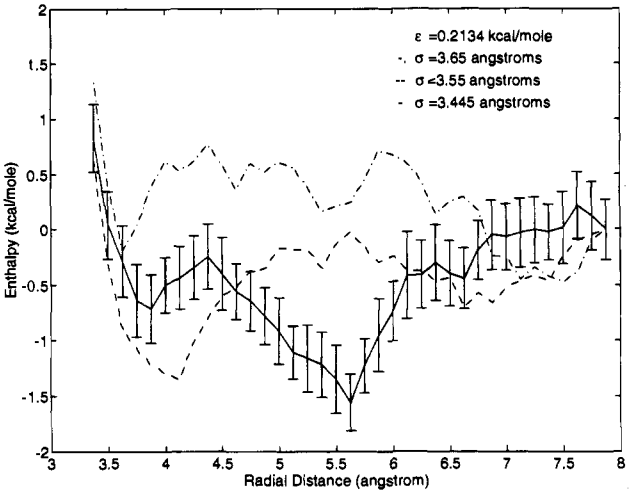

Figure 5. The enthalpy of methane association in the $\lambda = 0.0$ reference fluid for $\epsilon_{MeO} = 0.2134$ kcal/mol and varying the σ_{MeO} interaction length parameters: (a) —, $\sigma_{MeO} = 3.445$ Å, (b) - - -, $\sigma_{MeO} = 3.55$ Å, and (c) -·-, $\sigma_{MeO} = 3.65$ Å.

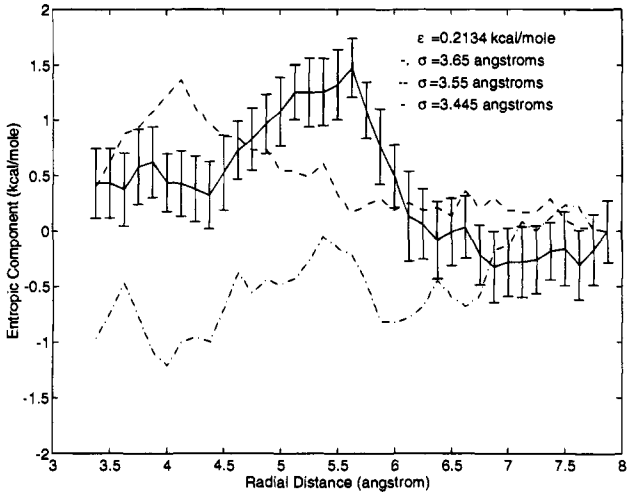

Figure 6. The entropic component ($-T\delta S$) of methane association in the $\lambda = 0.0$ reference fluid for $\epsilon_{MeO} = 0.2134$ kcal/mol and varying the σ_{MeO} interaction length parameters: (a) —, $\sigma_{MeO} = 3.445$ Å, (b) - - -, $\sigma_{MeO} = 3.55$ Å, and (c) -·-, $\sigma_{MeO} = 3.65$ Å.

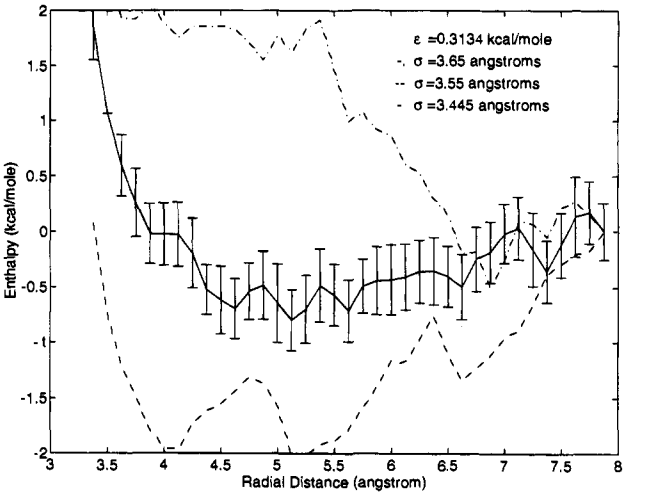

Figure 7. The enthalpy of methane association in the $\lambda = 0.0$ reference fluid for $\epsilon_{MeO} = 0.3134$ kcal/mol and varying the σ_{MeO} interaction length parameters: (a) —, $\sigma_{MeO} = 3.445$ Å, (b) - - -, $\sigma_{MeO} = 3.55$ Å, and (c) -·-, $\sigma_{MeO} = 3.65$ Å.

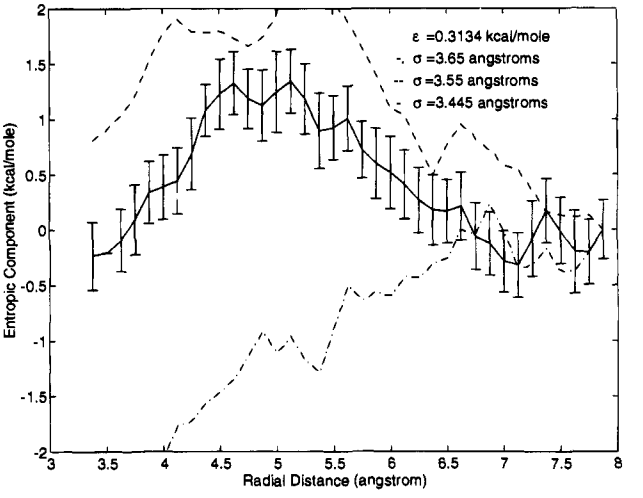

Figure 8. The entropic component ($-T\Delta S$) of methane association in the $\lambda = 0.0$ reference fluid for $\epsilon_{MeO} = 0.3134$ kcal/mol and varying the σ_{MeO} interaction length parameters: (a) —, $\sigma_{MeO} = 3.445$ Å, (b) - - -, $\sigma_{MeO} = 3.55$ Å, and (c) -·-, $\sigma_{MeO} = 3.65$ Å.

$\sigma_{MeO} = 3.445$, 3.55, and 3.65 Å, respectively. Figures 7 and 8 display the same sets of data, but with $\epsilon_{MeO} = 0.3134$ kcal/mol. One encouraging feature of the reference fluid is that its convergence characteristics for these difficult to converge properties are clearly superior as compared to previous fully hydrogen bonding water studies.[27,28] Fully coupled Φ_1 water studies by Smith and Haymet reached the conclusion that the contact region is entropically stabilized, using the SPC water model, 106 water molecules, and methane−oxygen parameters of $\sigma_{MeO} = 3.445$ Å and $\epsilon_{MeO} = 0.2134$ kcal/mol.[27,28] Their errors were too large too assign an entropic or enthalpic origin to the free energy barrier and solvent-separated minimum.[27,28] Their free energy profile, and the free energy profile generated with ST4 as the water solvent model, is most similar to our reference fluid simulation with $\sigma_{MeO} = 3.65$ Å and $\epsilon_{MeO} = 0.2134$ kcal/mol. We have reached the same qualitative conclusions on the enthalpy and entropy breakdown of the free energy at the contact minimum. Therefore, we take this as further confirmation that the reference fluid is behaving sensibly in a thermodynamic sense.

For σ_{MeO} values of 3.55 Å or less, in which there is a change in the energy ordering of the two minima to prefer the solvent-separated region (which also occurs in Φ_1 models of solvent for values of σ_{MeO} between 3.2 and 3.445 Å), there seems to be a reversal in the thermodynamic driving forces at the solvent-separated minimum. To a first approximation the trends in the entropy are the same for both parameter sets, where the contact minimum is entropically stabilized relative to the barrier region. There is a reversal of entropic trends in which the solvent-separated minimum is entropically stabilized relative to the barrier in the case of the smaller interaction length parameter, while it appears to be destabilized relative to the barrier in the case of the larger σ_{MeO} value; the still significant error bars (±0.3 kcal/mol) make the latter assignment in relative entropies tentative. For the enthalpy, the contact and solvent-separated regions are destabilized with respect to the barrier for small σ_{MeO}, while just the opposite holds for large σ_{MeO}. The mechanism of hydrophobic effect seems to change as the methane−water interaction length decreases beyond a certain value, since there is a reversal in the thermodynamic roles of enthalpy and entropy. The view that reduction of hydrophobic surface area entropically drives the solutes into contact seems incomplete, since the observed thermodynamics would be more understandable if small changes in solute−water interactions

also altered the way in which solvent−solvent interactions developed around the solutes. One surmises that there may be a distinct solvent structure which allows for greater optimization of solvent−solvent interactions around the individual, separated solutes, in spite of the greater amount of surface area the two separate hydrophobic entities would now expose to solvent.[41] Once a critical solute−water interaction length is reached, however, a different structuring around the solutes in contact is the more viable option. The structural basis, if any, for the qualitative change in the thermodynamic behavior as a function of methane−water parameters will be the subject of a forthcoming paper.[47]

5. Conclusions and Future Directions

This paper introduces a new Hamiltonian for approximating water solutions containing hydrophobic groups and has verified its ability to reproduce thermodynamic trends for methane association in water as compared to the ST4 model,[35] semi-empirical PC theory,[20,22] and previous fully hydrogen bonding water model simulations.[21,23−28] These trends include (1) a preference for the contact minimum once a large enough value of the methane−water interaction length parameter, σ_{MeO}, is reached and a shift of the barrier and solvent-separated minimum position to larger r,[20,27,28] (2) increasing preference for the solvent-separated minimum as ϵ_{MeO} is increased,[20] and (3) entropic stabilization of the contact minimum for large σ_{MeO}.[1−3,27,28] We have also shown for the first time that the reversal in the ordering of the free energy minima for small decreases in σ_{MeO} is due to a reversal of roles in entropy and enthalpy at the solvent-separated minimum. The reversal in thermodynamic trend occurs over such a small range in σ_{MeO} that simple structural pictures of entropically driven reductions in surface area are unsatisfying.[1−3,27,28] Such small changes in solute−solvent interaction suggest that a more complete analysis must include the mechanism by which solvent−solvent interactions respond to changes in the solute−solvent interactions.

The primary discrepancy between our reference fluid and ST4 water model simulations is the effective size of water in its interaction with methane, where an increase of ~0.2 Å in this parameter is necessary to reproduce all trends. Simulation results of pure water using the reference fluid and the ST4 model showed that both fluids contain triads of oxygens forming equilateral triangles, although the isotropic fluid shows a greater amount of such structure than its ST4 counterpart.[35] The greater number of non-tetrahedral triads in the reference fluid (which are energetically unfavorable with respect to the tetrahedral angles) make solvent−solvent interactions a little weaker and orientationally ambiguous on average when compared to Φ_1 models. This implies that the reference fluid can accommodate a slightly larger cavity size (i.e. a larger σ_{MeO}) than fully-hydrogen-bonded models before "squeezing" the solutes into contact.[16−19] We emphasize again that this same phenomena occurs for Φ_1 models, but at smaller absolute values of σ_{MeO}. We also mention that improvements in the analysis of neutron diffraction indicate the $g_{OO}(r)$ as originally reported over-emphasized the height and narrowness of the first peak. Reformulation of our reference fluid using the new $g_{OO}(r)$ data may very well reduce the amount of defect structure in the Φ_0 model.[48]

Acknowledgment. This work was supported by the Office of Health and Environmental Research, Office of Energy Research, Department of Energy, under contract No. DE-AC03-76SF00098. Acknowledgment is made to the National Energy Research Supercomputer Center for Cray time. Thanks to Sienny Shang for help with the figures and to Dr. Frank H. Stillinger for enjoyable discussions.

JA941328T

(47) Shang, H. S.; Head-Gordon, T. Manuscript in preparation.

(48) Soper, A. K. Private communication.